International Journal of Computational and Experimental Science and ENgineering
(IJCESEN)

Vol. 11-No.3 (2025) pp. 4029-4035
http://www.ijcesen.com

ISSN: 2149-9144

Research Article

Improved Optical System Design of Human Eye Using Ant Colony Optimization

Suha Mousa Khorsheed[1], Nissan S. Oraibi[2], Wildan Mohammed Awad[3], Mohammed Sahib Mahdi Altaei[4]

[1]Department of Physics, College of Science, Al-Nahrain University, Jadriya, Baghdad, Iraq
* **Corresponding Author Email:** suha.korsheed@nahrainuniv.edu.iq - **ORCID:** 0000-0002-9544-3677

[2]Department of Physics, College of Science, Al-Nahrain University, Jadriya, Baghdad, Iraq
Email: Nissan.oribi@nahrainuniv.edu.iq - **ORCID:** 0000-0001-8484-1162

[3]Department of Physics, College of Science, Al-Nahrain University, Jadriya, Baghdad, Iraq
Email: wildan.awad@nahrainuniv.edu.iq - **ORCID:** 0000-0001-6269-6339

[4]Department of Computer Science, College of Science, Al-Nahrain University, Jadriya, Baghdad, Iraq
Email: mohammed.sahibmahdi@nahrainuniv.edu.iq - **ORCID:** 0000-0001-8749-2973

Article Info:

DOI: 10.22399/ijcesen.2691
Received : 27 February 2025
Accepted : 25 May 2025

Keywords

OSD
Human Eye Simulation
Optimization
ACO
Evolutionary Algorithms

Abstract:

The motive we address in this paper is to design an accurate optical system for the human eye using a newly used approach based on optimizing a human eye model by the Ant Colony Algorithm (ACO). The optimization process dealt with the optical features of both the cornea and the lens. The optimal model of the eye was obtained after 100 cycles, in each of which a specific number of ants are placed that secrete the pheromone at each movement. This method allows the ant to make 1000 movements. The initial evaluation of the improvement process showed that the objective function led the ants to improve the selection of the values of the optical features, and that the improvement approached the optimal limits at the last ant turns. The optimal eye model resulting from the optimization was tested by quality measures: OTF and spot size, and were found to be very close to optimal values, which indicating efficiency of evolutionary methods for achieving the intended optical design of the human eye.

1. Introduction

Traditional optical system design (OSD) is associated with imaging systems such as cameras, where unique features and capabilities are often required to improve the performance of designed system to be used in a specific particular application. Optical design first needs to analyze the OSD characteristics according to how the application may be practiced in the fields of visual systems, imaging system, or even the communication systems [1]. The human eye is considered one of the most important models of visual system, and work the on analyzing and designing the optical model of the human eye is one of the most important researches because it is an ideal and complex behavioral structure that cannot be manufactured because. In this paper, we develop and improve a model of the human eye according to the design proposed in [2] depending on evolutionary methods. The shape of the human eye is a ball-like shape with a diameter of about 22*mm*. Inside the eye, there are light-sensing sensors at the retina in the inner back surface. The purpose of the eye being spherical is to ensure its movement within the eye cavity in all directions and at a few specific angles. The human eye is not a perfect sphere, as there is a slightly greater convexity at the front that makes the radius of curvature smaller than the total curvature, and is necessary to make plane wave rays passing through an eye fluid with a refractive index close to water converge on the retina. [3]. Figure (1) shows a vertical cross-section of the human eye components, the schematic diagram in the figure shows that the eye consists of four main parts [4]: the cornea, the iris and the pupil, eye lens, and then the retina.

The cornea is a hard, transparent membrane that is more curved, and is the first surface on which light entering the eye falls. The cornea is an elongation with the sclera representing the tough white outer shell of the eye. The transparency of the cornea is

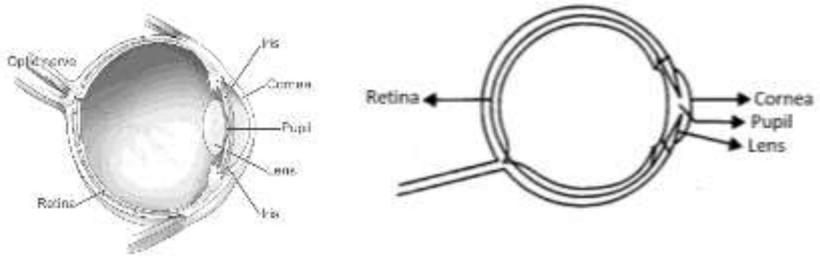

Figure 1. *Human eye configuration [4].*

due to the regular arrangement of the layers of collagen fibers that make up most of the thickness of the cornea [5,6]. The continuous closing of the eyelid maintains the moisture of the outer surface of the cornea and makes its surface smooth when light is refracted. Changes in the thickness of the tear film may lead to scattering and diffraction of the optical rays [7]. The average refractive index of the cornea is about 1.376, and its thickness in the center is about 0.5 to 0.6 mm, and the average radius of curvature for its first surface is 6.5 to 7.7*mm*. [8, 9]. The iris and pupil are the second component of the eye after the cornea. The iris is a membrane that gives the eye its color characteristics. The pigment in the iris is either blue, green, gray or brown and is present in the aqueous humor. The pupil controls the amount of light entering the eye, which plays an important role in image quality and vision. At high levels of illumination, the size of the pupil is small in order to stop the most deflecting peripheral rays, while the size of the pupil is large at low levels of illumination to allow the entry of more photons of light and equalize the signal-to-noise ratio, so the image becomes clearer, the average diameter of the pupil be between 3 and 4*mm* [10]. The lens of the eye consists of a crystalline material in the form of a fibrous gel capsule. The lens is more rigid in its center and gradually decreases at the edges. Muscular ligaments hold the lens in place. The refractive index of the lens ranges between 1.383 in the periphery and 1.420 in the center, which is one of the most important optical constants for the natural lens of the eye, while the radius of curvature of the front of the lens is 7 to 8 mm and the rear is - 5.5 to - 6 mm, and the thickness of the lens in its normal state is 2.5 mm [11]. The retina is the inner membrane of the eye that contains photoreceptors. Photoreceptors are of two types: rods and cones. The retina contains a large number of neurons that transmit signals originating in the visual receptors to the brain. Inside the eye cavity, there is an aqueous mixture in the anterior chamber between the iris and the lens, with an aqueous refractive index of 1.333. There is also a vitreous humor in the second chamber between the retina and the lens that resembles a jelly called the vitreous humor, which is a transparent substance with a refractive index of 1.336 [12,13].

2. ACO for Improving OSD

Ant colony optimization (ACO) was inspired by the behavior of real ants in order to find optimal solutions for many applications, where it was found that ants have the ability to find the shortest paths between the food source and the anthill [14]. This is done when the ant puts a chemical called a pheromone along its path. In the absence of this pheromone, the ant moves randomly, but when the pheromone is present, the rest of the ants infer their path and follow the path of the pheromone.
Experiments indicate that ants go towards pheromones of high concentration, and that each ant walking in this path secretes an additional pheromone to increase the pheromone concentration in the path. This method allows discovering the shortest path to food. And after a while, the pheromone evaporates the paths that are no longer passable for the fun, so they are neglected. This behavioral phenomenon of ants is used to be adapted as an optimization method useful in obtaining promising solutions using ACO [15]. The ant colony algorithm was first proposed by Dorigo and colleagues as a multi-agent approach for solving difficult combinatorial optimization problems such as the quadratic assignment problem (QAP) and the traveling salesman problem (TSP) [16]. Today there are many scientific researches based on the application of the ant colony algorithm in order to obtain improved solutions to existing problems, such as routing in the communication network [17], graph coloring [18] and the vehicle routing problem (VRP) [19, 20].
In the ant colony optimization algorithm, the method has n cycles, in each of which: m ants construct a simple solution as a first step, after which each ant visits all nodes and applies a pheromone. Improved solutions are subsequently formed by incorporating knowledge other ants have gathered in the past about good decision solutions. To illustrate this, suppose an ant is located at node *i*

as shown in Figure (2), to choose the next node *j* that has not yet been visited by that ant, there are two stochastic strategies can be chosen [21]:

1. Narrow heuristic: Choose one priority role like nearest random neighbor. The resolution for all nodes *j* is dependent on the inverse of the distance between nodes *i* and *j*. Then the ant moves to the next node randomly according to the probabilities determined by those decision values. Consequently, if node *j* is closer to *i* than *g* or *k*, then the ant is almost moving to node *j* and the constructive inference decision values are called *ij*.
2. Pheromone trails: When ants walk in different directions, the ants release a specific amount of pheromone. The pheromone concentration increases with the number of ants that follow this path. When there are several choices an ant can take, it prefers the path with the highest pheromone concentration. According to this strategy, the initial amount of pheromone is zero for all pathways (*i*, *j*). The pheromone concentration is then updated for each cell of the track after the ant completes the round. The pheromone amount τ_{ij} of the path (*i*, *j*) represents the desire of the ant to choose to move to node *j* when it is standing at node *i*. Therefore, good solutions receive a large amount of pheromone. The probability that ant *v* in node *i* will fall into the next node *j* is determined by the following formula:

$$P_{ij}^{v} = \begin{cases} \dfrac{(\tau_{ij})^{\alpha}(\eta_{ij})^{\beta}}{\sum_{k=1}^{N_i^v}(\tau_{ik})^{\alpha}(\eta_{ik})^{\beta}} & if\ j \ni N_i^v \\ 0 & Otherwise \end{cases} \quad (1)$$

where, α and β are given weighting factors, N_i^v is the node set that have not yet been visited by the ant currently located at *i* node.

The application of the ant colony algorithm to improve the performance of optical systems depends on creating an initial optical model, and then forwarding a number of ants equal to the number of optical characteristics for each element in the OSD (such as curvature). There are two possible paths for the ant to follow: towards increasing the amount of curvature, or towards decreasing the amount of curvature. The ant's decision at first is random, but becomes regular after n loops with increasing amount of pheromone. The amount of the increase or decrease is determined by a certain initial value, then it changes to half the value when the ant finds that it has exceeded the optimal solution. The ants continue to search and deposit the pheromone until the optimal solutions are obtained [22, 23].

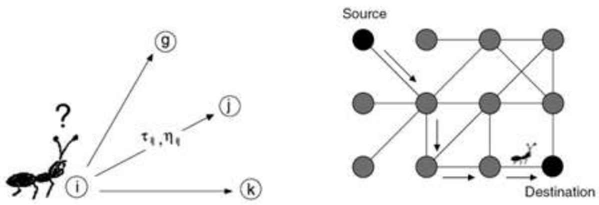

Figure 2. *Possible paths may choose by the ant [21, 23].*

3. Related Work and Contribution

There is a small number of literature that dealt with the process of improving the visual system of the human eye, while there is a lot of literature that dealt with the subject of eye design. Recent research discusses the issue of understanding the harmony between the optical elements of the eye by estimating performance using approved optical measures. The following is an illustration of the most important research dealing with the area of interest.

3.1 Related Work

Many papers have been published that involve making models of the human eye in a modern way, and one of the most important of these published papers is the designing of Human Eye in [24]. In this research, the design of an optical system for the retinal camera is carried out based on the Schack-Hartmann sensor in order to use it as a wavefront detector, and the liquid crystal spatial light modulator was used as a wavefront corrector to correct the high-order aberrations of the human eye. Different scopes were used in the lighting system during the shoot. The results show that the illumination light strongly deflects the reflected light of the cornea and can illuminate the human eye uniformly. In [25], an optical coherence tomography system is designed for simultaneous zoom imaging of the cornea and retina. This design can also image the entire eye. An electrically adjustable lens with a zoom response time of 15 ms and a specific optical delay line was used. Cross-scan ranges were used to within 8 mm in the full-eye scan and 14 mm in the single-frame fast scan. The system with electrically adjustable lens and optical delay line has realized full eye depth imaging in vivo. In [26], an OPD-Scan III thermometer (Nidek) was used to determine total, corneal, and internal ocular aberrations. Two groups were used: one with congenital anisotropic myopia and the other with acquired myopia. The results showed that the axial length of the eye with higher myopia was greater than the length of the fellow eye. This prepared for the detection of increased asphericity and astigmatism in the cornea in the eyes with higher myopia of patients with congenital myopia compared to acquired myopia. In [27], The work concerns a method for extending on-axis modeling of an individual eye to the peripheral retina. Measurements of axial distances, central visual quality, and corneal geometry of some subjects' eyes were used. In order to reproduce the peripheral visual quality of the eye, a crystalline lens model was designed for a single eye model representing the average eyes of 25 participants. A prediction of the individual visual peripheral quality was obtained over the central 40 degree range, which made it possible to compare the results of the final model with the actual measurements of the peripheral visual quality of the participants. The results showed that there was a significant agreement between the visual quality measures measured for the final model with regard to astigmatism and relative spherical valence. In [28], scanner performance is optimized for a cost-effectively reconfigurable beam based on three electrically adjustable lenses. Which gives the lenses the ability to control the focus, the angle of incidence, and the position of the beam. Thus, this lens can be used for alternate imaging of the rear and front parts by alternating the parallel angular beam scanning instead of the focused beam scanning. OCT images of the whole eye were recorded as well as experimented in a rabbit eye ex vivo. The beamwidth scanner used reduced the cost and complexity of other whole-eye scanners and was compatible with two-dimensional ocular biometrics. The added versatility of visual inspection reconfiguration has been found to help extend the service of use to other ophthalmic applications and beyond.

3.2 Problem Statement and Contribution

The use of optimization to model the human eye system design (HESD) by OSD concepts is not an easy process because of many optical parameters that have to be taken into account, each optical element possesses optical properties: radius of curvature (R_1, R_2), refractive index (n), diameter (D), thickness (t), inter-between distance (d), as well as the refractive index of both the aqueous (n_a) and the vitreous (n_v). In order to overcome the problem of changing the pupil with lighting and changing the curvature of the lens with the distance of the object, it is possible to choose the optimal values for the optical qualities of the components of the eye so that the image formed in the retina is clearly obvious, and the performance of the designed eye is efficient. The contribution depends on the optimization of the visual characteristics of the eye by the ant colony optimization algorithm, which is an evolutionary method for the automation of the finite state by controlling a continuous change of the values of the visual characteristics by means of a directive function.

4. Proposed HESD Method

The proposed method is based on making an eye model as a preliminary project based on the known constants of the eye, then it is improved by the ACO algorithm to obtain the best design that matches the real eye. This requires going through two stages: the initial eye-making stage, and the improvement stage. Here is a detailed explanation of each of these two phases:

4.1 HESD Modeling

The human eye consists mainly of two changeable optical components, the cornea and the lens. While the rest of the parts are fixed and do not affect the process of refracting the light rays entering the eye. Such that, the pupil diameter is set to be 3.5*mm*. Also, the materials that affect the refraction of rays in the eye are fixed, including the transmission media of rays such as the vitreous body, while the retina is a plate that contains light sensors that enable the vision of the image of objects.

Table 1. *The default values of the initial eye model [3, 4].*

Ser.	Optical Element	Optical Feature	Min. Value	Max. Value
1	Cornea	R_1	6.5mm	7.7mm
		R_2	6.5mm	7.1mm
		t	0.5mm	0.6mm
		D	8.13mm	8.23mm
		d	3.2mm	3.6mm
		n_o	1	1
		n_1	1.376	1.376
		n_2	1.333	1.333
2	Iris	No determined optical features		
3	Pupil	D	3*mm*	4*mm*
4	Lens	R_1	7mm	8mm
		R_2	-5.5mm	-6.1mm
		t	2.482mm	2.517mm
		D	6.92mm	7.112mm
		d	0.625mm	0.645mm
		n_o	1.333	1.333
		n_1	1.38	1.38
		n_2	1.336	1.336
5	Retina	No determined optical features		

Therefore, the main parameters that determine the efficiency of eye performance are those parameters of the cornea and lens of the human eye, in which the refractive indices must be the same values as in the real eye. Table (1) shows a prototype of the eye design, showing that some parameters are fixed and

Table 2. *Optimal optical features of improved HESD by ACO.*

Optical Element	***Optical Features***							
	Variable					***Fixed***		
	R_1	***R_2***	***t***	***D***	***d***	***n_o***	***n_1***	***n_2***
Cornea	6.82541	6.72864	0.54826	8.16287	3.57269	1	1.376	1.333
Eye lens	7.72692	-5.82692	2.49273	7.09265	0.63892	1.333	1.38	1.336

some are variable within a specific change range that does not exceed the realistic values of the real eye. Figure (3) shows the locations of these parameters on the eye design schematically.

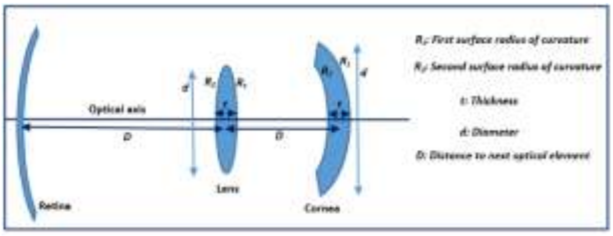

Figure 3. *Optical system scheme of human eye design [Ref].*

4.2 ACO of HESD Model

The eye model given in Table (1) was used according to the constraints of each optical feature between the lowest and the largest value in the optimization process by ACO. Where two groups of ants are placed, each group consists of 8 ants, each ant deals with the process of improving one of the eight optical features of the visual element. Such that, the first group of ants is placed on the cornea to improve its optical features, while the second group of ants is placed on the lens for the same purpose. The fixed optical features in Table (1) do not allow the ant to move to neighboring places, and thus these features are remains fixed and unchanging, while the variable features take an initial value equal to the average value of change range, and allow the ant to move in the positive direction (increase in the value of the optical feature) or in the negative direction (decrease in the value of the optical feature) at a rate of change (g) of 0.00001 of the extent of change of that optical feature. The number of cycles (C) is set at 1000 cycles. In each cycle, the ant moves to a neighboring location according to the probability calculated from equation (1). After all cycles are over, new ants are placed in the same locations as the old ants, and they are given the opportunity to move and move according to the amount of pheromone of the ants of the previous cycle and the objective probability calculated from equation (1). After completing 100 ant laying operations (Ant turn: N=100), each is performing 1000 movements, the results that are most likely to be improved are evaluated.

5. Results and Discussions

The proposed approach of ACO applied on HESD was implemented by Python programming language. The designed software is addressed to find out the optimal HESD that can simulate the descriptive imaging performance of real-life eye. Throughout the implementation of ACO, no local minima occurred and the ants were always directed towards improvement. The results improved consequentially even achieving the optimal resulted design of the eye given in Table (2) that shown in Figure (4) schematically.

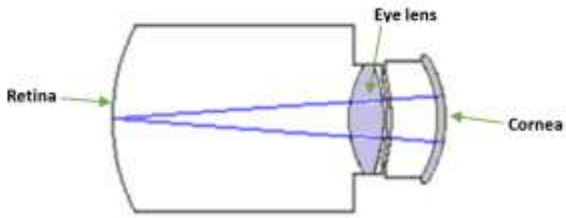

Figure 4. *Resulted optimal HEDS by ACO.*

Figure (5) shows the normalized optimization behavior that occurred in the used design of the eye, which is belong to the last optimization cycle of N = 100. It is noticeable that the improvement was not occur during the first turns of the ants because the random movement of the ants that overpowered the objective function that depended on a low concentration of the pheromone. After more than 5 ant turns, the ants' movement towards improving the optical features of the eye showed a bias, after the pheromone concentration increased with the ants' movements between allowed values of optical features positively. This bias made the improvement to be fast in the beginning, up to the ant turns of more than 20, where the improvement seemed less and gradual, this is due to the pheromone evaporation factor. Also, in this region, the behavior began to appear few fluctuations indicating the speed of making decisions to move the ants to new locations at the ends of the path of each ant. Where the new ant follows a path is defined by abundant pheromone till the end of defined path, and then it decides where to go with a next movement. It is observed that the fluctuations are relatively small, because it is corrected with new transitions depending on the objective function. And the process of gradual improvement continues with new ant turns till reaching the best situation at the 100th turn. We also note that the improvement did not match the ideal condition (improvement value = 1) due to specifying the value of accuracy by the amount of change (g = 0.00001). Reducing the value of g more will lead to additional improvement values approaching the optimal condition, but will not match ideal one, which also lead to slower arrival to optimal results.

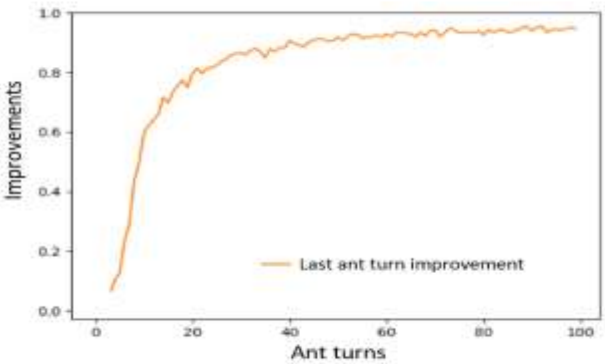

Figure 5. *Optimization improvements occurred in the optical properties of the handled human eye design.*

6. Results Evaluation

In order to evaluate the optimization results obtained by ACO, optical performance measures provided by Zymax software are used, Zymax software is a well-known tool for researchers in the design of optical systems, and it provides the possibility of evaluating the performance of optical systems, quantitatively and qualitatively. The OTF measure was chosen as a quantitative measure, and the spot separation measure was chosen as a qualitative measure to evaluate the performance of the resulted HESD developed by ACO.
The OTF is a measure of the amount of aberration and defocus in the optical system. Figure (6) shows the behavior of the OTF curve of the optimal design that we obtained by optimization with ACO compared to the ideal case. It is noted that the behavior of the OTF curve almost matches the optimal case. And the difference is due to the residual spherical aberration at the higher levels, which needs high optimization accuracy to treat it. Fortunately, this effect does not affect the quality of vision because it is less than the amount of spacing between any two sensors in the retina, and this makes the minimum deviation in the OTF and without any distortion of vision. The contrast of the OTF values gives the impression that the image formed in the eye is very clear, and therefore the performance of the enhanced eye is almost perfect compared to the real eye.

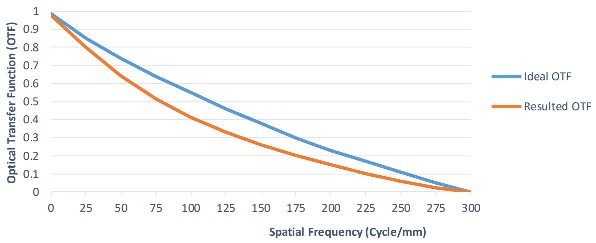

Figure 6. *Resulted OTF of the improved HESD by ACO.*

On the other hand, the size and shape of the macula formed on the retina were used to measure the imaging efficiency of HESD by ACO. Smaller spot size means less beam separation and sharper retinal image of higher resolution. In fact, the spot size of achieved optimal HESD invented by ACO was about 5μm with an effective focal length (EFL) of about 17mm, these values are roughly equivalent to those of an ideal eye. Figure (7) shows the spot diagram of the optimal design, which is very similar to the ideal case in which there is only diffraction in the imaging without aberration, which makes the light spot formed in the retina similar to the ideal case mentioned in [11] and without differences. This confirms the validity of the improvement results and the procedures followed.

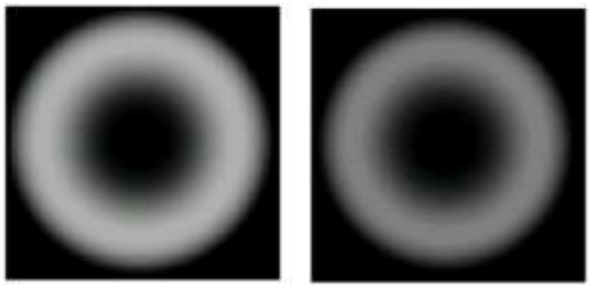
(a) Optimal spot. (b) Ideal spot.
Figure 7. *Spot diagram of improved HESD by ACO comparing with ideal one achieved by Zemax.*

7. Conclusions and Recommendations

In the current work, some important points were noted including: The process of improving optical systems by evolutionary methods is suitable for the purpose of developing the performance of optical models, such as the human eye. The process of improving the design of the human eye model produced a great resemblance to the real eye, the achieved values of EFL and spot size are proved the successful improvement of achieved human eye model to be similar to the ideal eye. The current work can be improved by dealing with a variable amount of lighting, taking into account the change in the pupil size with the amount of lighting, which gives the impression of simulation closer to reality.

Author Statements:

- **Ethical approval:** The conducted research is not related to either human or animal use.
- **Conflict of interest:** The authors declare that they have no known competing financial interests or personal relationships that could have appeared to influence the work reported in this paper
- **Acknowledgement:** The authors declare that they have nobody or no-company to acknowledge.
- **Author contributions:** The authors declare that they have equal right on this paper.
- **Funding information:** The authors declare that there is no funding to be acknowledged.
- **Data availability statement:** The data that support the findings of this study are available on request from the corresponding author. The data are not publicly available due to privacy or ethical restrictions.

References

[1] Wilson, J., & Hawkes, J. (1998). Optoelectronics: An Introduction (3rd ed.). *Prentice Hall Europe*.

[2] Bilteanu, L., et al. (2021). Human Eye Optics Within A Non-Euclidian Geometrical Approach And Some Implications In Vision Prosthetics Design. *Journal of Biomolecules*. 11;211-215. https://doi.org/10.3390/biom11020215

[3] Khorsheed, S. M., et al. (2011). Optical System Design For Human Eye Using Genetic Algorithm. *Iraqi Journal of Science*. 52(1);109-117. https://doi.org/10.24996/ijs.2011.52.1.%25g

[4] Navarro, R. (2009). The Optical Design Of The Human Eye: A Critical Review. *Journal of Optometry*. 2;3-18. https://doi.org/10.3921/joptom.2009.3

[5] Francois, G., et al. (2009). Image-Based Modeling Of The Human Eye. *IEEE Transactions on Visualization and Computer Graphics*. 15(5);815-827. https://doi.org/10.1109/TVCG.2009.24

[6] Sun, X. (2021). Design Of The Poster Image System Based On Human Vision. *Scientific Programming*. 2021;1411145. https://doi.org/10.1155/2021/1411145

[7] Watson, A. B. (1999). Digital Images And Human Vision. *The MIT Press*.

[8] Tkacik, G., et al. (2011). Natural Images From The Birthplace Of The Human Eye. *PLOS ONE*. 6(6). https://doi.org/10.1371/journal.pone.0020409

[9] Burt, P. J. (1989). Multiresolution Techniques For Image Representation, Analysis, And 'Smart' Transmission. In *Visual Communications And Image Processing IV* (pp. 2-15). *SPIE*. https://doi.org/10.1117/12.970014

[10] Yang, J., Meng, Q., Murroni, M., Wang, S., & Shao, F. (2020). IEEE Access Special Section Editorial: Biologically Inspired Image Processing Challenges And Future Directions. *IEEE Access*. 8;147459-147462. https://doi.org/10.1109/access.2020.3015372

[11] Ruan, H., Xu, J., & Yang, C. (2021). Optical Information Transmission Through Complex Scattering Media With Optical-channel-Based Intensity Streaming. *Nature Communications*. 12(1). https://doi.org/10.1038/s41467-021-22692-1

[12] Cheng, Lin, Liao, et al. (2019). Trace Gas Detection System Based On All-Optical Quartz-Enhanced Photoacoustic Spectroscopy. *Applied Spectroscopy*. 73(11);1327-1333. https://doi.org/10.1177/0003702819866468

[13] Kim, B. C., Ko, D., Jang, U., Han, H., & Lee, E. C. (2017). 3D Gaze Tracking By Combining Eye-And Facial-Gaze Vectors. *The Journal of Supercomputing*. 73(7);3038-3052. https://doi.org/10.1007/s11227-016-1817-5

[14] Yin, S., Zhu, M., & Liang, H. (2019). Multi-Disciplinary Design Optimization With Variable Complexity Modeling For A Stratosphere Airship. *Chinese Journal of Aeronautics*. 32(5);191-202. https://doi.org/10.1016/j.cja.2019.03.003

[15] Hassanalian, M., Salazar, R., & Abdelkefi, A. (2019). Conceptual Design And Optimization Of A Tilt-Rotor Micro Air Vehicle. *Chinese Journal of Aeronautics*. 32(2);159-171. https://doi.org/10.1016/j.cja.2018.10.006

[16] Yang, X., & Kim, Y. Y. (2018). Topology Optimization For The Design Of Perfect Mode-Converting Anisotropic Elastic Metamaterials. *Composite Structures*. 201;161-177. https://doi.org/10.1016/j.compstruct.2018.06.022

[17] Qiu, H., Fang, W., & Guo, B. (2020). A Layout Generation Algorithm For Unequal-area Display And Control Console Considering Ergonomics. *IEEE Access*. 8;29912-29921. https://doi.org/10.1109/access.2020.2971575

[18] Alhaag, M. H., & Ramadan, M. Z. (2017). Using Electromyography Responses To Investigate The Effects Of The Display Type, Viewing Distance, And Viewing Time On Visual Fatigue. *Displays*. 49;51-58. https://doi.org/10.1016/j.displa.2017.07.003

[19] Dorigo, M., & Stützle, T. (2019). Ant Colony Optimization: Overview And Recent Advances. In *Handbook of Metaheuristics* (pp. 311-351). *Springer International Publishing*. https://doi.org/10.5772/intechopen.111839

[20] Kleinkauf, R., Mann, M., & Backofen, R. (2015). Antarna: Ant Colony-Based RNA Sequence Design. *Bioinformatics*. 31(19);3114-3121. https://doi.org/10.1093/bioinformatics/btv319

[21] Gaifang, D., Xueliang, F., Honghui, L., & Pengfei, X. (2017). Cooperative Ant Colony-genetic Algorithm Based On Spark. *Computers & Electrical Engineering*. 60;66-75. https://doi.org/10.1016/j.compeleceng.2016.09.035

[22] Starzec, M., Starzec, G., Byrski, A., Turek, W., & Pietak, K. (2020). Desynchronization In Distributed Ant Colony Optimization In HPC Environment. *Future Generation Computer Systems*. 109;125-133. https://doi.org/10.1016/j.future.2020.03.045

[23] Altaei, M. S. M., et al. (2011). Ant Colony System With Median Based Partitioning For Image Segmentation And Classification. *Iraqi Journal of Science*. 52(2);247-258. https://doi.org/10.24996/ijs.2011.52.2.%25g

[24] Wang, D. D., et al. (2020). Design of a human eye retinal camera optical system with dual wavelength coaxial astigmatism correction. *Optical and Quantum Electronics*. 52;393-404. https://doi.org/10.1007/s11082-020-02472-9

[25] An, L., et al. (2021). Depth imaging through anterior to posterior segment of whole human eye based on optical coherence tomography in the spectral-domain. *OSA Continuum*. 4(11);156-164. https://doi.org/10.1364/osac.440686

[26] Neroev, V. V., et al. (2023). Anatomical and optical parameters and aberrations of the optical system of the eye in anisometropic myopia. *Russian Ophthalmological Journal*. 16(2);47-53. https://doi.org/10.21516/2072-0076-2023-16-2-47-53

[27] Tabernero, J., et al. (2023). Individualized modeling for the peripheral optics of the human myopic eye. *Biomedical Optics Express*. 14(6);216-225. https://doi.org/10.1364/boe.489792

[28] Urizar, P., et al. (2023). Optical beam scanner with reconfigurable non-mechanical control of beam position, angle, and focus for low-cost whole-eye OCT imaging. *Biomedical Optics Express*. 14(9);362-371. https://doi.org/10.1364/boe.493917